EPR Investigations of the Inactivation of *E. coli* Ribonucleotide Reductase with 2′-Azido-2′-deoxyuridine 5′-Diphosphate: Evidence for the Involvement of the Thiyl Radical of C225-R1

Wilfred A. van der Donk,[§,⊥] JoAnne Stubbe,[*,‡,⊥] Gary J. Gerfen,[†,§,⊥] Brendan F. Bellew,[†,§,⊥] and Robert G. Griffin[*,†,⊥]

Contribution from the Department of Chemistry, Department of Biology, and Francis Bitter Magnet Laboratory, Massachusetts Institute of Technology, Cambridge, Massachusetts 02139

Received May 11, 1995[⊗]

Abstract: Ribonucleotide reductase (RNR) from *Escherichia coli* catalyzes the conversion of nucleotides to deoxynucleotides and is composed of two homodimeric subunits: R1 and R2. 2′-Azido-2′-deoxyuridine 5′-diphosphate (N_3UDP) has previously been shown to be a stoichiometric mechanism based inhibitor of this enzyme. Inactivation of RNR is accompanied by loss of the tyrosyl radical on the R2 subunit concomitant with formation of a new nitrogen centered radical. The X-band EPR spectrum of this radical species exhibits a triplet hyperfine interaction of ~25 G arising from one of the three nitrogens of the azide moiety of N_3UDP and a doublet hyperfine interaction of 6.3 G which has been proposed to arise from a proton. High frequency (139.5 GHz) EPR spectroscopic studies of this nitrogen centered radical have resolved the peaks corresponding to all three principal *g*-values: $g_{11} = 2.01557$, $g_{22} = 2.00625$, and $g_{33} = 2.00209$. In addition, the nitrogen hyperfine splitting along g_{33} is resolved ($A^N_{33} = 31.0$ G) and upper limits (~5 G) can be placed on both A^N_{11} and A^N_{22}. Comparison of these *g*- and *A*-values with those of model systems in the literature suggests a structure for the radical, XN•SCH_2–, in which SCH_2 is part of a cysteine residue of R1, and X is either a nonprotonated sulfur, oxygen, or carbon moiety. Use of an *E. coli* strain that is auxotrophic for cysteine and contains the nucleotide reductase gene allowed [β-^{2}H]cysteine labeled RNR to be prepared. Incubation of this isotopically labeled protein with N_3UDP produced the radical signal without the hyperfine splitting of 6.3 G, indicating that this interaction is associated with a proton from the –SCH_2– component of the proposed structure. These results establish that the nitrogen centered radical is covalently attached to a cysteine, probably C225, of the R1 subunit of RNR. Site-directed mutagenesis studies with a variety of R1 mutants in which each cysteine (439, 462, 754, and 759) was converted to a serine reveal that X cannot be a substituted sulfur. A structure for the nitrogen centered radical is proposed in which X is derived from 3′-keto-2′-deoxyuridine 5′-diphosphate, an intermediate in the inactivation of RNR by N_3UDP. Specifically, X is proposed to be the 3′-hydroxyl oxygen of the deoxyribose moiety.

Introduction

Ribonucleotide reductases (RNRs) catalyze the conversion of nucleotides to deoxynucleotides.[1,2] Despite the diversity of metallocofactors that can be utilized in this reduction process, a common mechanism has been proposed involving three essential active site cysteines.[1,3] Two cysteines (C225 and C462 in the aerobic *E. coli* reductase) have been postulated to provide the reducing equivalents for nucleotide reduction by electron and proton transfer reactions.[4,5] The third cysteine, C439, is postulated to be oxidized to a thiyl radical which initiates nucleotide reduction by 3′-hydrogen atom abstraction from the nucleotide substrate.[3,6] In the *E. coli* reductase this activity resides on the homodimeric R1 subunit. The second subunit of the *E. coli* RNR, R2, contains a diferric cluster and tyrosyl radical[7] that is proposed to initiate nucleotide reduction by a series of long range coupled electron and proton transfer reactions to R1 which generates the thiyl radical on C439.[6] This model is supported by the recent structure determinations of the R1 and R2 subunits.[8–10] The studies on the R1 subunit reveal that the three cysteines described above are within 6 Å of one another and furthermore that 225 and 462 are present in this structure as a disulfide.[8] While mechanisms involving thiyl radicals have been postulated, only recently with the RNR from *Lactobacillus leichmannii* has direct evidence in support of this model been provided.[11]

A number of approaches can be used to obtain evidence in support of this model. The most definitive approach would be to directly observe such species by EPR spectroscopy. Alter-

* Corresponding authors.
† Francis Bitter Magnet Laboratory.
‡ Department of Biology.
§ These authors contributed equally to this work.
⊥ Department of Chemistry.

[11] Abbreviations: EPR, electron paramagnetic resonance; RNR, ribonucleotide reductase; N_3UDP, 2′-azido-2′-deoxyuridine 5′-diphosphate; ESEEM, electron spin echo envelope modulation; DTT, dithiothreitol; Tris, tri(hydroxymethyl)aminomethane; ATP, adenosine 5′-triphosphate; TTP, thymidine 5′-triphosphate; NADPH, reduced β-nicotinamide adenine dinucleotide phosphate; TR, thioredoxin; TRR, thioredoxin reductase; 3′-ketodUDP, 3′-keto-2′-deoxyuridine 5′-diphosphate; LB, Luria broth.

⊗ Abstract published in *Advance ACS Abstracts*, August 15, 1995.

(1) Stubbe, J. *Adv. Enzymol. Relat. Areas Mol. Biol.* **1990**, *63*, 349–417.
(2) Reichard, P. *Science* **1993**, *260*, 1773–1777.
(3) Stubbe, J. *J. Biol. Chem.* **1990**, *265*, 5329–5332.
(4) Mao, S. S.; Holler, T. P.; Yu, G. X.; Bollinger, J. M.; Booker, S.; Johnston, M. I.; Stubbe, J. *Biochemistry* **1992**, *31*, 9733–9743.
(5) Åberg, A.; Hahne, S.; Karlsson, M.; Larrson, Å.; Ormö, M.; Åhgren, A.; Sjöberg, B. M. *J. Biol. Chem.* **1989**, *264*, 2249–2252.
(6) Mao, S. S.; Yu, G. X.; Chalfoun, D.; Stubbe, J. *Biochemistry* **1992**, *31*, 9752–9759.
(7) Sjöberg, B.-M.; Reichard, P.; Gräslund, A.; Ehrenberg, A. *J. Biol. Chem.* **1977**, *252*, 536–541.
(8) Uhlin, U.; Eklund, H. *Nature* **1994**, *370*, 533–539.
(9) Nordlund, P.; Sjöberg, B.-M.; Eklund, H. *Nature* **1990**, *345*, 593–598.
(10) Nordlund, P.; Eklund, H. *J. Mol. Biol.* **1993**, *232*, 123–164.
(11) Licht, S. S.; Stubbe, J. *FASEB J.* **1995**, *9*, A1320.

0002-7863/95/1517-8908$09.00/0 © 1995 American Chemical Society

Scheme 1

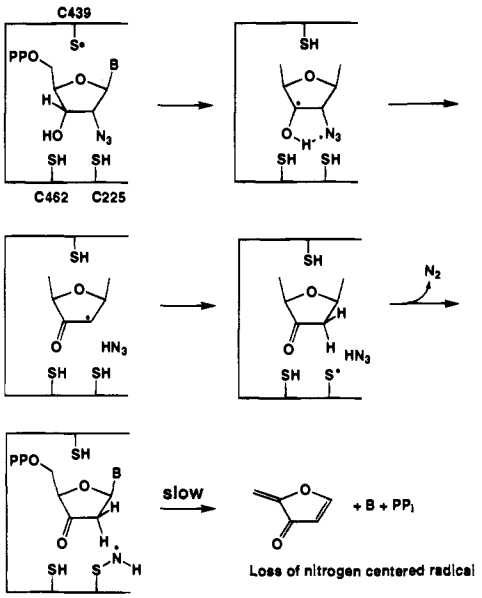

natively, to obtain a persistent radical more amenable to study by EPR methods, a radical trap could be built into the substrate if the active site of the enzyme can accommodate substrate flexibility. In the case of RNR, it was established in 1976 by Thelander, Eckstein, and their collaborators that 2′-azidodeoxynucleotides are potent mechanism based inhibitors of this enzyme.[12] Detailed studies of this process have revealed that approximately 1 equiv of inhibitor results in the complete inactivation of the enzyme[13] and that this process is accompanied by rapid destruction of the essential tyrosyl radical on the R2 subunit and concomitant formation of a new relatively stable nitrogen centered radical.[14,15] The nitrogen centered radical has been characterized by X-band EPR spectroscopy and shown to be composed of a 1:1:1 anisotropic triplet arising from interaction with a single nitrogen ($A^N = 25$ G) and a second hyperfine interaction possibly derived from a proton ($A^H = 6.3$ G).[14,15] Deuterium labeling experiments in D_2O,[14,15] with [^{2}H]-labeled R2[14] and with N_3UDP [^{2}H]-labeled at the 1′, 2′, 3′, and 4′ positions,[16] however, have failed to reveal the source of the proton hyperfine interaction. The inactivation process is initiated by 3′-carbon–hydrogen bond cleavage, evidenced by ^3H_2O release from [3′-^{3}H]N_3UDP and is accompanied by rapid loss of 1 equiv of N_2.[13] Decay of the relatively stable nitrogen centered radical occurs over a much longer period of time ($t_{1/2}$ = 10 min) and is accompanied by complete destruction of N_3-UDP resulting in the formation of uracil, inorganic pyrophosphate, and 2-methylene-3(2*H*) furanone.[13] Based on the postulated mechanism for nucleotide reduction, a mechanism for the mode of inactivation of RNR by N_3UDP has recently been proposed (Scheme 1).[16,17] Support for this mechanism was provided by studies with the C225SR1 mutant which revealed that while the nucleotide is decomposed in a fashion analogous to that observed with the wt-RNR resulting in uracil and furanone formation, no tyrosyl radical loss or nitrogen centered radical formation was detected. Instead azide ion or radical was observed.[16] In addition, when [2′-^{13}C]N_3UDP was incubated with wt-RNR, the spectrum of the nitrogen centered radical revealed no hyperfine interaction with the ^{13}C nucleus. These results establish that the 2′-carbon–nitrogen bond is cleaved and strongly implicate C225 as a key player in the conversion of some form of azide to N_2 and a nitrogen centered radical.

The present study describes our successful efforts using high frequency EPR spectroscopy together with RNR containing [β-^{2}H]cysteine to provide evidence that the nitrogen centered radical is covalently bound to the sulfur of a cysteine of the R1 subunit of RNR. A novel structure is proposed in which an initial nitrogen centered radical HN•S_{Cys225}R1, not detected experimentally, reacts further with the 3′-keto-2′-deoxynucleoside 5′-diphosphate (3′-ketodUDP) produced during this incredible sequence of events to generate the RNR S_{Cys225}N•X(dUDP) structure (Scheme 4).

Results and Discussion

140 GHz EPR Spectrum of the Nitrogen Centered Radical. While the amount and identity of the products generated during the interaction of RNR with N_3UDP have been determined, the structure of the new nitrogen centered radical has remained elusive.[13–16] In the past few years, the feasibility of applying high frequency EPR spectroscopy to the investigation of the structures of protein-associated free radical species has been realized.[18–22] In particular, our study of the tyrosyl radical of *E. coli* RNR, in which principal *g*-values and hyperfine coupling constants were determined,[22] laid the groundwork for the present high frequency EPR investigation of the relatively stable nitrogen centered radical. As in earlier studies, incubation of N_3UDP with RNR for 8 min produced a mixture of both the tyrosyl radical and the nitrogen centered radical. The 139.5 GHz EPR spectrum (first harmonic saturated dispersion) of this mixture, shown in Figure 1A, was subjected to a pseudomodulation algorithm to yield Figure 1B (see Experimental Methods). This signal is composed of approximately 66% nitrogen centered radical, 32% tyrosyl radical, and 2% resonator-based impurity. To obtain the spectrum of the nitrogen centered radical (Figure 1E), subtractions of the remaining tyrosyl radical (Figure 1C) and a signal originating from the impurity (Figure 1D) were carried out. As anticipated, subsequent to these manipulations, peaks associated with all three principal *g*-values of the nitrogen centered radical are resolved ($g_{11} = 2.01557$, $g_{22} = 2.00625$, and $g_{33} = 2.00209$). In addition, information concerning the nitrogen hyperfine coupling in an axis system defined by the principal axes of the g-matrix is obtained. The hyperfine splitting along g_{33} is resolved and is measured to be = 31.0 G. Although not resolved, an upper limit of ~5 G can be placed on splittings along g_{11} and g_{22} based on the line widths of the peaks associated with these *g*-values. The assignment of these splittings to ^{14}N is further supported by the high frequency EPR

(12) Thelander, L.; Larsson, B.; Hobbs, J.; Eckstein, F. *J. Biol. Chem.* **1976**, *251*, 1398–1405.
(13) Salowe, S. P.; Ator, M.; Stubbe, J. *Biochemistry* **1987**, *26*, 3408–3416.
(14) Sjöberg, B.-M.; Gräslund, A.; Eckstein, F. *J. Biol. Chem.* **1983**, *258*, 8060–8067.
(15) Ator, M.; Salowe, S. P.; Stubbe, J.; Emptage, M. H.; Robins, M. J. *J. Am. Chem. Soc.* **1984**, *106*, 1886–1887.
(16) Salowe, S. P.; Bollinger, J. M., Jr.; Ator, M.; Stubbe, J.; McCracken, J.; Peisach, J.; Samano, M. C.; Robins, M. J. *Biochemistry* **1993**, *32*, 12749–12760.
(17) A second, minor pathway in which the substrate radical intermediate is quenched from the top face by C439 also occurs.[16]
(18) Prisner, T. F.; McDermott, A. E.; Un, S.; Norris, J. R.; Thurnauer, M. C.; Griffin, R. G. *Proc. Natl. Acad. Sci. U.S.A.* **1993**, *90*, 9485–9488.
(19) Bowman, M. K.; Thurnauer, M. C.; Norris, J. R.; Dikanov, S. A.; Gulin, V. I.; Tyrshkin, A. M.; Samoilova, R. I.; Tsvetkov, Y. D. *Appl. Magn. Reson.* **1992**, *3*, 353–368.
(20) Burghaus, O.; Plato, M.; Bumann, D.; Neumann, B.; Lubitz, W.; Möbius, K. *Chem. Phys. Lett.* **1991**, *185*, 381–386.
(21) Gulin, V. I.; Dikanov, S. A.; Tsvetkov, Y. D.; Evelo, R. G.; Hoff, A. J. *Pure Appl. Chem.* **1992**, *64*, 903–906. Un, S.; Brunel, L.-C.; Brill, T. M.; Zimmermann, J.-L.; Rutherford, W. A. *Proc. Natl. Acad. Sci. U.S.A.* **1994**, *91*, 5262.
(22) Gerfen, G. J.; Bellew, B. F.; Un, S.; Bollinger, J. M., Jr.; Stubbe, J.; Griffin, R. G.; Singel, D. J. *J. Am. Chem. Soc.* **1993**, *115*, 6420–6421.

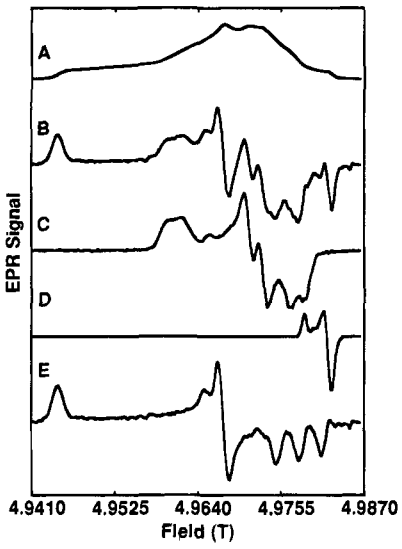

Figure 1. High-frequency EPR spectra of the incubation mixture containing N_3UDP and RNR (A) Saturated modulation-detected (first harmonic) dispersion signal of 340 μM R1, 280 μM R2, incubated for 8 min with 1.0 mM N_3UDP; (B) Pseudomodulation (first harmonic) of the experimentally acquired EPR signal depicted in (1A) (see experimental methods); (C) Experimentally acquired EPR spectrum of the tyrosyl radical (Y_{122}•) in the R2 subunit subsequent to pseudomodulation (first harmonic); (D) EPR spectrum of the resonator-based paramagnetic impurity following pseudomodulation; (E) Isolated spectrum of the nitrogen-centered radical remaining after subtraction of fractional amounts of normalized Y_{122}• signal (32%) and of normalized resonator-based-impurity signal (2%) from the spectrum depicted in (1B). All EPR spectra were acquired under the following conditions: microwave frequency, 139.5 GHz; temperature, ~10 K; microwave power ~20 μW; modulation amplitude, 2.4 G; modulation frequency, 400 Hz; scan rate, ~0.3 G/s; time constant 1 s.

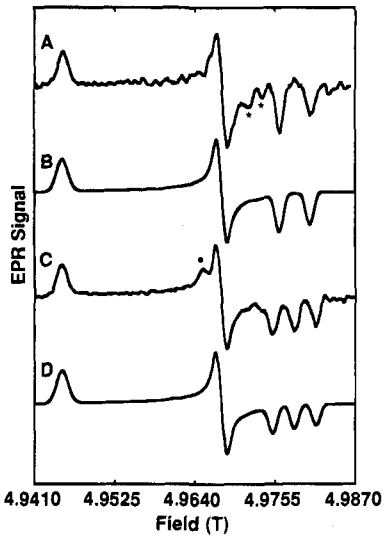

Figure 2. High-frequency EPR spectra of the nitrogen-centered radical formed by inhibition of RNR with N_3UDP. (A) Spectrum of [^{15}N]-nitrogen-centered radical formed upon incubation of R1 and R2 with [$^{15}N_3$]N_3UDP after subtraction of the signal from the tyrosyl radical. The spectrum is a numerical pseudomodulation of an experimentally acquired saturated dispersion spectrum. Asterisks mark artifactual features arising from imperfect subtraction of the Y_{122}• signal; (B) Simulation using the parameters listed in Table 1, entry 12 and Table 2, entry 4; (C) Spectrum of the nitrogen-centered radical arising from incubation of [^{14}N]-N_3UDP with RNR after subtraction of the tyrosyl radical; (D) Simulation of (2C) using the parameters listed in Table 1, entry 12 and Table 2, entry 3. Asterisk marks an extraneous signal from a paramagnetic impurity which was not completely eliminated upon spectral subtraction.

spectrum of the radical species generated when the inactivation was carried out using [^{15}N]N_3UDP (Figure 2). The collapse of the high field 1:1:1 triplet into a 1:1 doublet together with the change in the observed hyperfine splitting from 31.0 to 43.4 G is consistent with the substitution of the ^{14}N ($I = 1$) azido group of N_3UDP with an ^{15}N azido group ($I = 1/2$, with the ratio of magnetic moments of ^{15}N and ^{14}N equal to 1.40).

Possible Structures based on the Results from the High Frequency EPR Experiments. The magnitude and anisotropy of the g-values and the nitrogen hyperfine coupling, together with the relative orientation of the principal axes of these interactions, suggest that this species is a π-type nitrogen radical with the structure [XN•SR].[23-29] Table 1 shows EPR data for some known nitrogen based radicals in which a portion of the unpaired electron density is delocalized onto adjacent sulfur or oxygen atoms. Structures such as [R′(NO•)R″][23] and [R′N•-OR″][24] can be eliminated from consideration since the smaller spin-orbit coupling constant of oxygen relative to sulfur yields g-values (g_{iso} = 2.0044−2.0055, *e.g.*, Table 1, entries 1−3) well below those measured here (g_{iso} = 2.00797, entry 12). Structures such as [R′(NO•)SR″] can also be eliminated as they typically yield isotropic ^{14}N hyperfine splittings (15.4−18.3 G, *e.g.*, entry 4, Table 1)[25] significantly larger than the upper limit determined by the high frequency data (13.6 G) and the final value obtained through simulations of 9 GHz spectra (11.7 G, Table 1, entry 12, and Figure 3). The structures [R_2NS•] and [R_2NS•=O] have been detected as transient radicals at low temperatures and can be eliminated both on the basis of their chemical stability and their measured spectral parameters (entries 5 and 6).[26] Finally, studies of persistent radicals with the structures [R′N•SR″] (entries 7−9)[25] and [R′SN•SR″] (entries 10, and 11 in Table 1 and Table 2)[27-29] have shown that these compounds exhibit g-values and nitrogen hyperfine splittings remarkably similar to those determined in this study.[30] These high frequency EPR results are thus consistent with a structure [XN•SR] (X = sulfur- or carbon-based moiety) and provide a base from which additional questions concerning the identity of the radical can be addressed.

[β-2H]Cysteine RNR with N_3UDP: Evidence That the Nitrogen Centered Radical Is Covalently Bound to a Cysteine of R1. As outlined in the introduction, [^{2}H]-labeling of N_3UDP, solvent, or the R2 subunit of RNR failed to reveal the source of the proton hyperfine interaction with the nitrogen centered radical. Our most recent hypothesis (Scheme 1) for the formation of this radical thus suggested that it must be covalently bound to a cysteine of R1. As outlined above, the assignment of the radical structure as [XN•SR] from our high frequency EPR results supports this postulate. To further test this hypothesis, N_3UDP was incubated with R1 prepared in an *E. coli* strain auxotrophic for cysteine in which [β-^{2}H]cysteine was used to satisfy this auxotrophy. The EPR spectra at 9 GHz

(23) Libertini, L. J.; Griffith, O. H. *J. Chem. Phys.* **1970**, *53*, 1359−1367; *Spin Labeling*, Berliner, L. J., Ed., Academic Press: New York, 1976.
(24) Kaba, R. A.; Ingold, K. U. *J. Am. Chem. Soc.* **1976**, *98*, 7375−7380.
(25) Miura, Y.; Asada, H.; Kinoshita, M.; Ohta, K. *J. Phys. Chem.* **1983**, *87*, 3450−3455.
(26) Baban, J. A.; Roberts, B. P. *J. Chem. Soc., Perkin Trans. 2* **1978**, 678−683.
(27) Rolfe, S.; Griller, D.; Ingold, K. U.; Sutcliffe, L. H. *J. Org. Chem.* **1979**, *44*, 3515−3519.
(28) Harrison, S. R.; Pilkington, R. S.; Sutcliffe, L. H. *J. Chem. Soc., Faraday Trans. 1* **1984**, *80*, 669−689.
(29) Preston, K. F.; Sandall, J. P. B.; Sutcliffe, L. H. *Magn. Reson. Chem.* **1988**, *26*, 755−759.
(30) Preston, K. F.; Sutcliffe, L. H. *Magn. Reson. Chem.* **1990**, *28*, 189−204.

Table 1. Comparison of Isotropic EPR Parameters of Previously Reported Nitrogen Based Radicals and the Radical Obtained upon Incubation of RNR with N_3UDP

entry	Compound	R′	R″	g_{iso}	A^N_{iso} (G)	$A^{H_{R'}}_{iso}$ (G)	$A^{H_{R''}}_{iso}$ (G)	ref
1	R′(NO•)R″	*t*-Bu	*t*-Bu	2.0059	15.1			23
2	R′N•OR″	$PhCH_2$	$PhCH_2$	2.0046	14.4	23.8	2.6	24
3		H	$PhCH_2$	2.0049	12.2	20.1	3.2	24
4	R′(NO•)SR″	*t*-Bu	*n*-Bu	2.0071	18.3			25
5	R'_2NS•	Et		2.0156	10.7	6.1		26
6	R'_2NS•=O	Et		2.0060	6.1	2.3		26
7	R′N•SR″	*t*-Bu	*t*-Bu	2.0074	12.3			25
8		*n*-Bu	*t*-Bu	2.0073	12.4	15.4		25
9		*t*-Bu	*n*-Bu	2.0075	12.1		3.1	25
10	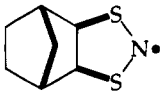			2.0064	13.1	3.5		27
11	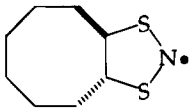			a	12.6	5.1		30
12	N• from RDPR and N_3UDP			2.00797[b]	11.7[c]	6.3		this work

[a] Not reported. [b] Calculated from $(g_{11} + g_{22} + g_{33})/3$ obtained from the 140 GHz EPR data. [c] calculated from $(A^N_{11} + A^N_{22} + A^N_{11})/3$ obtained from the 140 GHz EPR data.

Table 2. Anisotropic EPR Parameters of Previously Reported Nitrogen Based Radicals and the Radical Obtained upon Incubation of RNR with N_3UDP

entry	Compound	g_{11}	g_{22}	g_{33}	A^N_{11} (G)	A^N_{22} (G)	A^N_{33} (G)	ref
1	PhSN•SPh	2.0130	2.0077	2.0021	1.9	1.4	30.3	28
2		2.0136	2.0050	2.0023	2.4	2.2	30.2	29
3	N• from RDPR and N_3UDP	2.01557	2.00625	2.00209	2.0	2.0	31.0	this work[a,b]
4	N• from RDPR and [$^{15}N_3$]-N_3UDP	2.01557	2.00625	2.00209	2.8	2.8	43.4	this work[a,b]

[a] Adequate fits of experimental spectra are obtained using coincident g and A^N principal axes. [b] Uncertainties in g- and A^N-values are estimated to be 0.000 05 and 0.2 G, respectively.

resulting from this experiment and a control with [β-^{1}H]cysteine-RNR prepared by the same procedure are shown in Figure 4. In both cases the presence of the nitrogen centered radical and the tyrosyl radical are apparent. However, it is also readily apparent that the proton hyperfine interaction has finally been eliminated. Subtraction of the tyrosyl radical component from the spectrum in Figure 4B reveals the spectrum in Figure 4C. These results (Figure 4A compared with Figure 4B and Figure 3 compared with Figure 4C,D) establish unambiguously that the nitrogen centered radical is covalently attached to a cysteine of R1. Our previous site-directed mutagenesis studies using mutants of R1 (C225 and C462) indicate that C225 is a likely candidate for this cysteine.[16]

The 6.3 G splitting which is observed in X-band spectra of the [β-^{1}H] cysteine-RNR species (Figures 3 and 4A) is not resolved in the 139.5 GHz spectra (Figures 1 and 2). This may be explained by the fact that the high frequency spectra were obtained under conditions of saturation[31,32] (see Experimental Methods). Saturation leads to broader lineshapes[33] which may mask small hyperfine splittings. In addition, field dependent inhomogeneous and/or homogeneous broadening may also contribute to increased line widths in the high frequency spectra.[34]

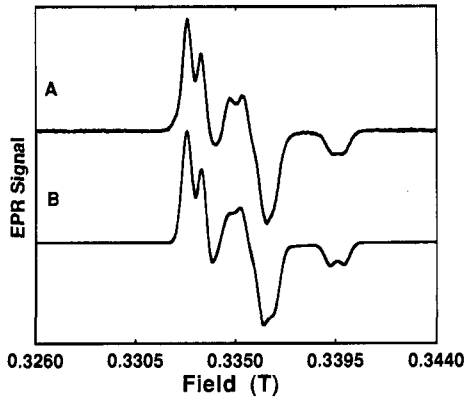

Figure 3. X-band EPR spectra of the nitrogen-centered radical formed by inhibition of RNR with N_3UDP; (A) EPR spectrum of nitrogen centered radical present in 8 min time point after subtraction of remaining tyrosyl radical. Experimental conditions are as follows: microwave frequency, 9.428 GHz; temperature, 100 K; power, ~1 mW, modulation amplitude, 1.5 G; modulation frequency, 100 kHz; time constant, 0.126 s; (B) Simulation of (3A) using parameters listed in Table 1, entry 12 and Table 2, entry 3.

Is the Nitrogen Centered Radical Covalently Bound to a Second Cysteine? The spectral parameters determined from

(31) Portis, A. M. *Phys. Rev.* **1953**, *91*, 1071.
(32) Dalton, L. R. In *EPR and Advanced EPR Studies of Biological Systems*; CRC Press: Boca Raton, 1985.
(33) Poole, C. P. *Electron Spin Resonance: A Comprehensive Treatise on Experimental Techniques*; Wiley: New York, 1983.

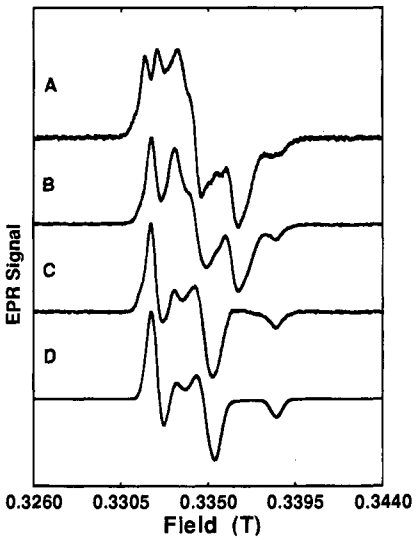

Figure 4. X-band EPR spectra of the nitrogen centered radical which indicates that the 6.3 G doublet arises from a cysteine proton. Instrument settings for all spectra were: power 1 mW, modulation amplitude 1.5 G, time constant 0.126 s, and temperature 101 K. (A) N_3UDP was incubated with RNR and the reaction was quenched after 8 min; (B) N_3UDP was incubated for 5 min with [β-^{2}H]cysteine RNR; (C) Isolated spectrum of the nitrogen centered radical remaining after 51% of a normalized Y_{122}• signal was subtracted from the spectrum depicted in (4B); (D) Simulation of the spectrum in (4C) based on the parameters listed in Table 1 (entry 12) and Table 2 (entry 3), except that 0.97 G was used for the ^{2}H-hyperfine splitting instead of the ^{1}H-hyperfine value listed in Table 1.

our high frequency EPR studies, when compared with data from model compounds (Tables 1 and 2), suggest that a second cysteine is a reasonable candidate for X in [XN•SR]. Furthermore, based on the extensive biochemistry carried out on R1, four additional cysteines are considered viable candidates: C462, C754, C759, and C439. Our previous studies[16] using C462SR1 revealed that this substitution had no effect on formation of the nitrogen centered radical and N_2. Thus the remaining candidates for the second cysteine in the structure [R′SN•SR″] are C439, C754, and C759. C439 is located on the β-face of the ribose ring, the face opposite from which the azide is released, and was anticipated not to play a role in this structure. In fact, incubation of C439SR1 RNR with N_3UDP resulted in no detectable chemistry,[16] consistent with its essential role in nucleotide reduction as the 3′-hydrogen atom abstractor. Given that either C754 or C759 are anticipated to be close in three-dimensional space to C225,[35] one of these cysteines appeared to be the most likely candidate for the second cysteine. Incubation of the double mutant C754S and C759SR1 with N_3-UDP was therefore examined. The results revealed that there was no effect on the nitrogen centered radical as determined by EPR spectroscopy (data not shown). Thus the results with the four cysteine site directed mutants of R1 imply that [R′SN•-SR″] is not a viable structure of the nitrogen centered radical.

Remaining Candidates for the Structure of the X Component of the Nitrogen Centered Radical. Our previously published hypothesis for the structure of this radical was that of [H′N•SCH$_2$R1] (Scheme 1).[16] Because this is a π-radical species with a large unpaired electron spin density on the nitrogen (as evidenced by the nitrogen hyperfine coupling), one would expect a significant hyperfine coupling to the α hydrogen (H′) for such a structure.[36] Ab initio calculations of a H′N•-SH″ radical determined a H′ isotropic hyperfine splitting of −24.13 G[25] via a spin polarization mechanism,[37,38] consistent with this expectation. Only one radical species claimed to be an [HN•SR] radical (R = Ar) has been reported in the literature.[39,40] These studies, however, make no mention of any proton hyperfine splittings and therefore cannot be used for comparison. However, the structurally and spectroscopically similar, isoelectronic species [H′N•OR″] have been studied and yield $|A_{iso}^{H'}| \approx 20$ G.[24] Because no splittings of this magnitude are observed in any of the spectra obtained for the nitrogen centered radical, the possibility of the structure being [HN•SR] needs to be reevaluated.[41] Thus, while we believe that this may be an intermediate in the formation of the observed nitrogen centered radical (Scheme 1), we now believe that the observed species must have a structure [−XN•SCH$_2$−] in which X is carbon or oxygen.

Compounds of the general structure [C′N•SC″] (Table 1, entries 7−9),[25] in which C′ and C″ are alkyl groups, have been reported to be remarkably stable radicals (lifetimes ranging from minutes to several hours at room temperature)[30] with g values and nitrogen hyperfine couplings very similar to those determined by high field EPR spectroscopy. We will first address the possibility of the presence of a proton bound to C′, that is, [H$_\beta$C′N•SC″]. Hyperfine couplings to β protons in π radical species arise primarily from a hyperconjugation mechanism[36,42−44] which, for [H$_\beta$C′N•SC″] systems, can be modeled by the equation[25]

$$A_{iso}^{H\beta} = \varrho_N(C + D\cos^2\theta) \sim \varrho_N D\cos^2\theta \sim 32.8\cos^2\theta \quad (1)$$

where ϱ_N is the spin density on the nitrogen, C and D are constants, and θ is the dihedral angle between the β proton and the nitrogen 2p$_z$ orbital. The constant C is typically small and therefore neglected,[45] while a value for $\varrho_N D$ of 32.8 G is obtained from solution state EPR spectra of [CH$_3$N•SC(CH$_3$)$_3$] for which splittings of $A_{iso}^{H\beta} = 16.4$ G were measured for three equivalent protons, and the time-averaged value of $\cos^2\theta = 0.5$ was taken for the freely rotating methyl group.[25] A reasonable upper limit on the size of an unresolved isotropic hyperfine splitting consistent with the observed 9 GHz spectra is approximately 3 G (Figures 3 and 4). Using eq 1, if a proton

(34) Lebedev, Y. S. in *Modern Pulsed and Continuous-Wave Electron Spin Resonance* Kevan, L., Bowman, M. K., Eds.; John Wiley & Sons, New York, 1990; pp 365−436.

(35) Lin, A. I.; Ashley, G. W.; Stubbe, J. *Biochemistry* **1987**, *26*, 6905−6909.

(36) Carrington, A.; McLachlan, A. D. *Introduction to Magnetic Resonance*; Harper & Row: New York, 1967, Wertz, J. E.; Bolton, J. R. *Electron Spin Resonance: Elementary Theory and Practical Applications*; Chapman and Hall: New York, 1986.

(37) McConnell, H. M.; Chesnut, D. B. *J. Chem. Phys.* **1958**, *28*, 107.

(38) McConnell, H. M.; Strathdee, J. *Mol. Phys.* **1959**, *2*, 129.

(39) Schmidt, U.; Kabitzke, K. H.; Markau, K. *Angew. Chem., Int. Ed. Engl.* **1964**, *3*, 373.

(40) Atkinson, R. S.; Judkins, B. D.; Khan, N. *J. Chem. Soc., Perkin Trans. 1* **1982**, 2491−2497.

(41) Sulfur tends to remove more spin density from the nitrogen than does oxygen, which would lead to smaller values for the H′ α proton hyperfine coupling in the H′NSR″ versus the H′NOR″ species. However, as is evident by comparison of nitrogen hyperfine coupling constants for R′NSR″ and R′NOR″ species (Table 1), the decrease in nitrogen spin density, and thus in the α proton hyperfine interaction, would be expected to be small (14%). Hyperfine interactions on the order of 15−17 G expected for H′NSR″ species would be observable if present.

(42) McLachlan, A. D. *Mol. Phys.* **1958**, *1*, 233.

(43) Heller, C.; McConnell, M. H. *J. Chem. Phys.* **1960**, *32*, 1535.

(44) Derbyshire, W. *Mol. Phys.* **1962**, *5*, 225−231.

(45) The spin density at the β-proton (and hence the isotropic hyperfine coupling $A_{iso}^{H\beta}$) is proportional to the degree of overlap between the sp^3-hybridized orbital on the β−carbon (C′sp^3) and the nitrogen 2p$_\pi$ orbital. This interaction has an angle independent contribution from the C′2s orbital (gauged by the constant C in eq 1) and an angle dependent contribution from the C′2p orbital (gauged by D); since the C′2p orbital is mainly responsible for this overlap, the constant C is much smaller than D (<10%) and is often neglected.[25,44]

β to the nitrogen were present in the radical, its dihedral angle would be restricted to $\theta = 90° \pm 17°$ to yield a hyperfine coupling of 3 G or less and account for the lack of resolution of this splitting in our spectra. Thus, if X in the radical structure [XN•SC″] is carbon, then this carbon must have either no protons bound to it or a proton whose dihedral angle is approximately 90 degrees with respect to the nitrogen $2p_z$ orbital.

We have been unable to find any studies on radicals of the type [X′ON•SR″], so this general structure cannot be eliminated based solely on EPR parameters. However, in the structurally similar species [R′CH_2SN•SCH_2R″], hyperfine couplings of the methylene protons have been measured to be 3−5 G,[30] indicating that appreciable spin density is delocalized onto the sulfur atoms.[46] Thus, the structure [H′SN•SR″] and analogously [H′ON•SR″] would be expected to give rise to an α-proton (H′) splitting of at least several gauss. As this proton would be expected to be exchangeable, differences in the EPR spectra of a radical species with this structure prepared in D_2O compared to the species in H_2O should be discernible. Such deuterium exchange experiments have been reported by us and by others.[14,15] Although the EPR spectral line widths are slightly narrower when the reaction is carried out in D_2O, the magnitude of the narrowing is too small to be explained by the exchange of a proton which experiences a hyperfine coupling of several G. Thus, we believe that [H′ON•SR″] is not a viable structure to accommodate the available data. Therefore, based on our EPR data we conclude that the radical is likely to have the structure [−XN•SCH_2−], in which the sulfur is derived from C225 of R1, and X is either an oxygen with no bound proton, or a carbon with no bound protons or one proton oriented approximately 90° with respect to the nitrogen $2p_z$ orbital.

Postulated Mechanism. The mechanism of nucleotide reduction postulates the importance of a number of transient thiyl radicals in catalysis.[1,3] Although EPR spectroscopy has been used and claimed to successfully detect thiyl radicals, the assignment of many of these observed signals to thiyl radical structures has been questioned.[47,48] The controversy results from the extreme reactivity of thiyl radicals which makes them difficult to trap before they react to form more stable sulfur-based radicals such as disulfide radicals or disulfide radical anions.[49] Furthermore, if the thiyl radical is successfully trapped, its EPR spectrum may be broad and difficult to detect, particularly in randomly oriented (frozen solution) samples. The difficulty arises from the near degeneracy of the p-π orbitals in which the unpaired electron is localized in thiyl radicals.[47,50] Because electronic orbital angular momentum is ineffectively quenched, this near-degeneracy causes the g-value which lies perpendicular to these orbitals (along the axis of the sulfur and its bonded partner) to be large and exquisitely sensitive to the surrounding environment.[47,48] The magnitude of, and the potential for a distribution in, this g-value may give rise to a broad EPR spectrum which is difficult to observe in randomly oriented solids. Rapid spin−lattice relaxation rates may also contribute to spectral broadening and hinder detection.[50]

Scheme 2

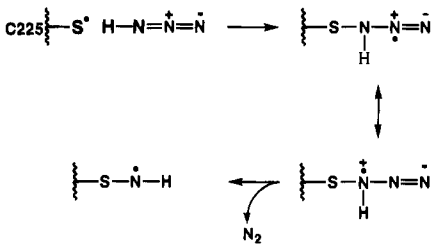

Scheme 3

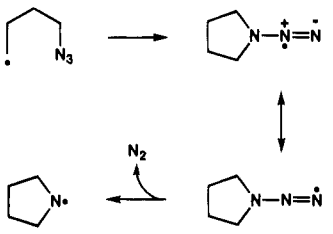

A general method to resolve this detection problem is the use of spin traps which convert an unstable radical into a persistent radical. While N_3UDP was not anticipated to be such a spin trap, it has been shown to serve in such a capacity.[14,15] High frequency EPR spectroscopy and the use of R1 containing [β-^{2}H]cysteine residues have provided the first support that a cysteine radical can be generated by RNR. Loss of the tyrosyl radical on the R2 subunit of RNR is believed to be accompanied by formation of a thiyl radical on R1 at C439.[1,3] A complex sequence of transformations such as those postulated in Scheme 1 can eventually lead to a thiyl radical on C225 which generates the observed nitrogen centered radical. The first three steps in this postulated mechanism (Scheme 1) are similar to those previously proposed for the normal nucleotide reduction process.[1,3] It should be emphasized, however, that subtleties regarding electron and proton transfer steps in both the normal reduction process and the inactivation reaction with N_3UDP are at present speculative. The results do, however, establish that the nitrogen centered radical is covalently attached to a cysteine of R1, and mutagenesis studies allow us to favor C225 as the candidate of choice.[16] A mechanism for how HN•SR1, a putative precursor to the observed nitrogen centered radical, could be generated from HN_3 and a thiyl radical (Scheme 1) is shown in Scheme 2. Several recent model studies support the feasibility that a thiyl radical can react with an alkylazide (RN_3) and ultimately lead to loss of N_2, hence the choice of HN_3. Recent studies of Kim and co-workers have shown that a carbon centered radical can convert an alkyl azide into N_2 and a nitrogen centered radical (Scheme 3).[51] A second study of Shingaki has shown that the decomposition of aromatic azides is greatly accelerated by the presence of thiols in combination with radical initiators resulting in the liberation of N_2 and disulfide formation.[52,53] Unfortunately the details of the mechanism of this transformation are not known, but presumably a thiyl radical is initiating the process which results in N_2 release.[53] This second model system may be mechanistically analogous to the better characterized reaction of aryl azides with thiolates which

(46) Indeed, direct measurement of the ^{33}S isotropic hyperfine interaction in [PhSN• SPh] (Table 2, entry 1) yielded spin densities of 0.12−0.17 on each sulfur atom (A^{33S} = 3.9 G), (Miura, Y.; Kinoshita, M. *Bull. Chem. Soc. Jpn.* **1980**, *53*, 2395−2396 and ref 25) while for the cyclic *exo*-1,2-norbornyl-1′,3′,2′-dithiazolidin-2′-yl compound in entry 10 of Table 1 A^{33S} = 2.89 G has been reported.[27]

(47) Symons, M. C. R. *J. Chem. Soc., Perkin Trans. 2* **1974**, 1618−1620.

(48) Gordy, W. *Theory and Applications of Electron Spin Resonance*; West, W., Ed.; Wiley: New York, 1980.

(49) Thiyl radicals formed by irradiation at liquid helium temperatures of single crystals of amino acids and peptides have been detected and studied by EPR spectroscopy (see for example Budzinski, E. E; Box, H. C. *J. Phys. Chem.* **1971** *75*, 2564. Kou, W. W. H.; Box, H. C. *J. Chem. Phys.* **1976** *64*, 3060).

(50) Akasaka, K. *J. Chem. Phys.* **1965**, *43*, 1182−1184.

(51) Kim, S.; Joe, G. H.; Do, J. Y. *J. Am. Chem. Soc.* **1994**, *116*, 5521−5522.

(52) Shingaki, T. *Sci. Rep. Coll. Gen. Educ. Osaka Univ.* **1963**, *11*, 67−79.

(53) Shingaki, T. *Sci. Rep. Coll. Gen. Educ. Osaka Univ.* **1963**, *11*, 81−92.

generate amines and N_2 concomitant with disulfide formation.[54,55] Site directed mutagenesis studies presented here and previously[16] in which C462, C754, and C759 have been changed to serines, however, indicate that a second cysteine is not required for liberation of N_2 in our inactivation process (Scheme 2). Thus the model we presently favor is that [HN•S_{cys}R1] is an intermediate in the formation of the final nitrogen centered radical. This intermediate may be detectable by using rapid freeze–quench EPR methods,[56] and these studies are in progress.

As previously discussed, EPR studies and site-directed mutagenesis studies presented here together with published EPR studies of model compounds have led to the conclusion that the nitrogen centered radical must have the structure [XN•S_{cys}R1] in which X is an oxygen or carbon atom having no hydrogens attached or a carbon atom with a single hydrogen attached but oriented in a defined fashion. What species within the active site could be the candidate for X? Our previous kinetic and product analysis studies have revealed that, at the time that the nitrogen centered radical is generated, the nucleotide analog is most probably still intact.[13] Electron spin echo envelope modulation (ESEEM) spectroscopy indicates that N_3UDP is converted into a species we propose to be 3′-ketodUDP in which the 1′-hydrogen is 3.0 Å from the nitrogen centered radical and the 4′-hydrogen is 2.7 Å from the same radical.[16,57] As anticipated by the role of C439, the 3′-hydrogen is ≥5 Å from this radical and is not detected by ESEEM methods. The 2′-^{2}H interaction with the nitrogen centered radical was also not detected by ESEEM spectroscopy.[16,57] Thus we postulate that XN•S_{cys}R1 is sitting on the α face of the carbonyl group of the 3′-ketodUDP and that it can interact with the carbonyl of this ketone to generate either compound **A** or **B** (Scheme 4).[58] In both cases, based on model chemistry (Table 1) a relatively stable nitrogen centered radical would be generated with the appropriate *g*-values and hyperfine interactions. While there is precedent in the literature for R′N•R″ interacting with an imine,[51] analogous to the first step in Scheme 4 pathway *a*, to our knowledge there is no precedent for the subsequent hydrogen atom migration to produce **A**, or for the steps leading to structure **B**. The structure of the observed nitrogen radical has an additional constraint which must be met. Our previously published experimental data requires that subsequent to the reduction of the nitrogen centered radical (half-life of 10 min), the adduct must collapse back into a 3′-ketodUDP which can further collapse to form the observed products: uracil, pyrophosphate, and furanone.[13] This chemical requirement originally led us to favor pathway *a* of Scheme 4. However, molecular modeling studies indicate that the distance between the 2′-proton and the nitrogen in structure **A** must be <5 Å (see Experimental Methods), and hence this interaction should have been observed in previous ESEEM studies. As summarized above this interaction was not detected, and

(54) Cartwright, I. L.; Hutchinson, D. W.; Armstrong, V. W. *Nucleic Acids Res.* **1976**, *3*, 2331–2339.

(55) Staros, J. V.; Bagley, H.; Standring, D. N.; Knowles, J. R. *Biochem. Biophys. Res. Commun.* **1978**, *80*, 568–572.

(56) Bollinger, J. M. Jr.; Tong, W. H.; Ravi, N.; Huynh, B. H.; Edmonson, D. E.; Stubbe, J. *Methods Enzymol. 258*, in press.

(57) These distances were obtained after reevaluation of our previously reported ESEEM data from experiments performed with [1′-^{2}H]N_3UDP and [4′-^{2}H]N_3UDP.[16] During this reevaluation the limit for detecting an interaction between the nitrogen based radical and the deuterium labels was reassessed to be ≤5 Å.

(58) At present we cannot exclude the possibility that the X-moiety of [XN• S_{cys}R1] is derived from a protein residue of the R1 subunit. However, the same restrictions will apply on X (i.e. oxygen with no bound proton, or a carbon with no bound protons or one proton oriented approximately 90° with respect to the nitrogen $2p_z$ orbital), eliminating most protein residues in the active site.

Scheme 4

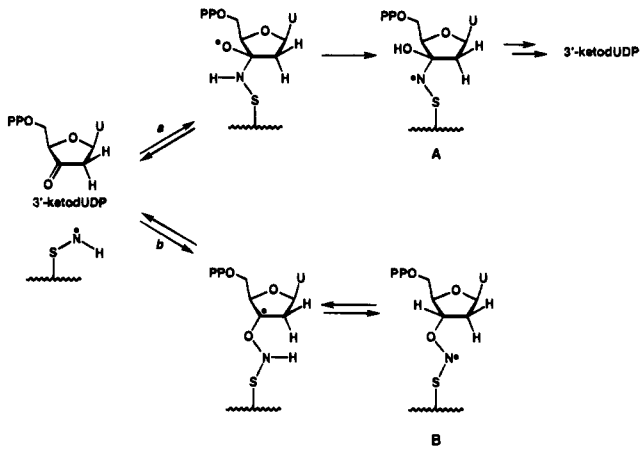

therefore structure **A**, while chemically appealing, is not a viable candidate for the nitrogen based radical. We are thus left with structure **B**. While this structure does in fact accommodate all of the spectroscopic data, the chemistry to arrive at this structure is, to our knowledge, not precedented. An isotopic labeling experiment in which N_3UDP is labeled at C-3′ with ^{17}O would perturb the EPR spectrum of the proposed structure in a predictable fashion and would thus allow us to obtain support for this model. Synthesis of this compound is being performed.

Conclusion

Regardless of the exact chemical nature of X in the [XN•S_{cys}R1] structure, the detailed studies of the N_3UDP dependent inactivation of RNR has given us an unprecedented glimpse into the amazing catalytic capabilities of this enzyme. The data establish for the first time that during this inactivation the nitrogen centered radical derived from the azide moiety of N_3UDP ends up covalently attached to a cysteine in the enzyme active site. Furthermore, isotopic labeling studies have unambiguously established that the observed 6.5 G hyperfine interaction detected many years ago by EPR spectroscopy[14] is due to a β-hydrogen of a cysteine in R1. The nitrogen centered radical is postulated to be generated via addition of a thiyl radical to HN_3 on the α-face of the bound nucleotide. Thus, this thiyl radical must be different from the thiyl radical on C439 postulated to initiate catalysis by hydrogen atom abstraction from the 3′-position of the nucleotide on its β-face. Site-directed mutagenesis studies of all conserved cysteines in R1 suggest that the thiyl radical trapped during inactivation is located on C225.

How does the generation of a thiyl radical on the α face of the substrate analog impact on our understanding of the normal nucleotide reduction process? The reducing equivalents in the reduction of NDP to dNDP are provided by the oxidation of C225 and C462 to a disulfide.[1,2] The reduction of a substrate derived intermediate in this complex process has been postulated to occur by a hydride transfer mechanism (2e$^-$ process) or two coupled one electron/proton or hydrogen atom transfer processes. Our studies with N_3UDP indicate the feasibility of this reduction occurring via one electron chemistry involving thiyl radicals.

Experimental Methods

General. R1 (ϵ_{280nm} = 189 000 M^{-1} cm^{-1}), specific activity 1400–1500 nmol min^{-1} mg^{-1}, and R2 (ϵ_{280nm} = 130 500 M^{-1} cm^{-1}), specific activity 7700–8000 nmol min^{-1} mg^{-1} were prepared as described

previously.[59] The R1-mutants were isolated from K38 overproducing strains according to literature procedures.[4,60] Cysteine auxotrophic *E. coli* strain JM15 (sex: F⁻; chromosomal markers: cysE50, tfr-8) was obtained from Dr. Barbara J. Bachmann, *E. coli* genetic Stock Center, Department of Biology, Yale University. Protein R1 and its analogs, prior to all EPR experiments, were prereduced at 25 °C for 20 min in the presence of 20 mM DTT. The excess DTT was removed by Sephadex G-25 chromatography. *E. coli* thioredoxin (TR) was isolated from the overproducing strain SK3981[61] with a specific activity of 36 units mg^{-1}, and thioredoxin reductase (TRR) was isolated from K91/pMR14[62] with a specific activity of 1000 units mg^{-1}. Adenosine 5′-triphosphate (ATP), thymidine-5′-triphosphate (TTP), and the chemically reduced form of β-nicotinamide adenine dinucleotide phosphate (β-NADPH) were obtained from Sigma. [3,3,3′,3′-^{2}H]-*d,l*-Cystine was purchased from Cambridge Isotopes. N_3UDP and [$^{15}N_3$]N_3UDP were prepared as described in previous work.[15,16] Quartz thick wall EPR tubes were employed for all 9.4 GHz EPR experiments. EPR spectra at 9 GHz were recorded on a Brüker ESP-300 spectrometer at 100 K. Spin quantitation was achieved with a 1.00 mM $CuSO_4$, 2 M $NaClO_4$, 0.01 M HCl, 20% (v/v) glycerol standard ($g = 2.18$).[63]

140 GHz EPR Experiments. The inactivation mixture contained 50 mM Hepes (pH 7.6), 15 mM $MgSO_4$, 1 mM EDTA, 340 μM R1, 280 μM R2, 1.0 mM NADPH, 10 μM TR, 0.5 μM TRR, 1.0 mM TTP and 1.0 mM N_3UDP in a final volume of 110 μL. Prior to the addition of the inhibitor to the reaction mixture, a sample was withdrawn corresponding to the $t = 0$ time point. The inhibitor was then added, and the reaction mixture was incubated at 25 °C for 8 min before being taken up in a fused silica sample tube (i.d. = 0.40 mm, o.d. = 0.55 mm) and frozen in liquid nitrogen. The EPR probe was cooled by immersion in liquid nitrogen and the sample tube was loaded into the cylindrical resonator of the EPR probe under liquid nitrogen. The probe was then placed inside the dewar which houses it, which had been previously cooled to a nominal temperature of 80 K; we estimate the temperature of the sample never exceeded 110 K.

EPR measurements were obtained at 139.500 GHz employing a homebuilt superheterodyne spectrometer with phase-sensitive detection.[64,65] The external magnetic field was swept from 49.410 to 49.870 kG at a scan rate of approximately 0.3 G/second. The external magnetic field was modulated at a frequency of 400 Hz by an amplitude of 2.4 G. Microwave power at the sample was approximately 20 μW which corresponds to a B_1 field approximately equal to 0.1 G. A steady flow of cold Helium gas maintained the sample at 8 K ± 0.5 K.

Under these experimental conditions, the EPR signals of both the nitrogen-centered radical and tyrosyl radical are saturated and exhibit adiabatic passage effects.[33] In particular, the absorptive component of the magnetic susceptibility is extremely small relative to the dispersive component.[66] Attempts were made to avoid saturation by obtaining spectra at low power levels (< 1 μW) and higher temperature, but this served only to decrease signal-to-noise ratios without appreciably affecting passage conditions. Thus, in order to maximize signal-to-noise ratios, published spectra were obtained under conditions which maximized the saturated first harmonic (modulation-detected) dispersion signal. Under these saturating conditions, modulation-detected dispersion signals have an "unconventional" appearance (similar to those of direct-detected, *i.e.* unmodulated, absorption signals[21,67]) and exhibit an increased line broadening and therefore decreased spectral resolution relative to conventional, unsaturated absorption signals.[33]

In order to improve resolution and achieve a more conventional representation (similar to that of modulation-detected absorption spectra), saturated dispersion spectra were subjected to pseudomodulation following the methods developed by Hyde *et al* .[68] In pseudomodulation, a computer algorithm operates on the recorded data to simulate the effect of an applied sinusoidal field modulation yielding the harmonics of that modulation; the algorithm also has the effect of acting as a digital noise filter.[68] Hyde *et al.*[68] calculate the *n*th harmonic of a spectrum using:

$$f_n(B_0,B_m) = FT^{-1}\{FT[f(B_0)]\cdot J_n(B_m S/2)\}$$

where f is the spectrum as recorded, f_n is its *n*th harmonic, B_0 is the external magnetic field, B_m is the pseudomodulation amplitude, FT is the Fourier Transform, J_n is the *n*th Bessel function, and S is the transform variable corresponding to B_0. We employ the equivalent, but more direct, calculation

$$f_n(B_0,B_m) = \int_{-1}^{+1} f\left(B_0 - \beta\frac{B_m}{2}\right)\cdot\frac{T_n(\beta)}{\sqrt{1-\beta^2}}d\beta$$

where β is a unitless variable of integration, and T_n is the *n*th Tchebyschev polynomial.

The external magnetic field was calibrated by recording the EPR spectrum of $Mn_{0.0002}Mg_{0.9998}O$ ($g = 2.00101$ and $A^{Mn} = 8.71$ mT);[69] measured values of the ^{55}Mn hyperfine sextet resonant fields were compared with values calculated with second-order corrections.

While the experimentally acquired spectra of the samples at $t = 8$ min are superpositions of $Y_{122}^{\bullet}$ signal and nitrogen-centered radical signal, analysis is most easily achieved when constituent signals are separate. Accordingly we have employed a spectral subtraction method in order to isolate the nitrogen-centered radical signal from the experimentally acquired spectra. For the purposes of this spectral subtraction, we acquired and processed identically an EPR spectrum of the $t = 0$ min sample, which exclusively consists of $Y_{122}^{\bullet}$ signal, and a spectrum of the empty EPR cavity which contained a slight amount of paramagnetic impurity. We then subtracted fractions of both the $t = 0$ min sample spectrum and the impurity spectrum from the $t = 8$ min spectrum; by parametric variation of the fractional amounts, we constructed difference spectra which were successively better approximations to the nitrogen-centered radical signal. Spectral regions characterized by distinctive features of $Y_{122}^{\bullet}$ signal overlaying relatively featureless parts of the nitrogen-centered radical signal served as sensitive indicators of successful isolation.

The correctness of the subtraction procedure was assessed, and the various magnetic coupling constants were determined, by comparison of all experimentally acquired spectra with detailed simulations. The simulation free parameters include three principal values of the *g*-matrix, three principal values of each hyperfine matrix, and relative orientations of each hyperfine matrix with respect to the *g*-matrix

$$B_{res}(\theta,\phi,m_I^1,\ldots,m_I^n) = \frac{h\nu_e}{g^{eff}(\theta,\phi)\beta} - \sum_{i=1}^{n} m_I^i A_i^{eff}(\theta,\phi) \quad (2)$$

where B_{res} is the resonant field, θ is the polar angle and ϕ is the azimuthal angle, h is Planck's constant, ν_e is the microwave frequency, $g^{eff}(\theta, \phi)$ is the orientationally dependent effective *g*-value, β is the Bohr magneton, and A_i^{eff} (in G) is the orientationally dependent hyperfine coupling to the *i*th nucleus. In the simulation of orientationally disordered samples 200 polar angles were sampled at equal intervals over a range of 0 to π. At each polar angle, between one and 400 azimuthal angles (the number being nearly equal to 400 times the sine of the polar angle) were sampled at equal intervals over a range 0 to 2π. At each orientation the resonant fields were calculated. The resulting distribution of resonant fields is convolved with a derivative

(59) Salowe, S. P.; Stubbe, J. *J. Bacteriol.* **1986**, *165*, 363–366.
(60) Mao, S. S.; Johnston, M. I.; Bollinger, J. M.; Stubbe, J. *Proc. Natl. Acad. Sci. U.S.A.* **1989**, *86*, 1485–1489.
(61) Lunn, C. A.; Kathju, S.; Wallace, B. J.; Kushner, S.; Pigiet, V. *J. Biol. Chem.* **1984**, *259*, 10469–10474.
(62) Russell, M.; Model, P. *J. Bacteriol.* **1985**, *163*, 238–242.
(63) Malmström, B.; Reinhammar, B.; Vänngård, T. *Biochem. Biophys. Acta* **1970**, *205*, 48.
(64) Becerra, L. R.; Gerfen, G. J.; Bellew, B. F.; Bryant, J. A.; Hall, D. A.; Inati, S. J.; Weber, R. T.; Un, S.; Prisner, T. F.; McDermott, A. E.; Fishbein, K. W.; Kreischer, K. E.; Temkin, R. J.; Singel, D. J.; Griffin, R. G. *J. Magn. Reson.*, accepted for publication.
(65) Prisner, T. F.; Un, S.; Griffin, R. G. *Isr. J. Chem.* **1992**, *32*, 357–363.
(66) Cullis, P. R. *J. Magn. Reson.* **1976**, *21*, 397.
(67) Ammerlaan, C. A. J.; Wiel, A. v. d. *J. Magn. Reson.* **1976**, *21*, 387–396.
(68) Hyde, J. S.; Jesmanowiscz, A.; Ratke, J. J.; Antholine, W. E. *J. Magn. Reson.* **1992**, *96*, 1–13.
(69) Burghaus, O.; Rohrerr, M.; Gotzinger, T.; Plato, M.; Mobius, K. *Meas. Sci. Technol.* **1992**, *3*, 765–774.

Gaussian line shape, whose width is also subject to parametric variation. This treatment proved adequate to reproduce the psuedomodulated saturated dispersion lineshape of the high-frequency spectra. In all cases a good fit was obtained assuming g-matrix principal axes to be coincident with nitrogen hyperfine matrix principal axes.

In order to assess the validity of the first-order treatment, we carried out additional simulations employing exact treatment of the nitrogen nuclear spin Hamiltonian (neglecting ^{14}N nuclear quadrupolar interaction) to calculate the resonant field and transition probability of each "allowed" and "forbidden" EPR transition. Simulations based on this more exact treatment were virtually indistinguishable from spectra calculated with eq 2, demonstrating the adequacy of the first-order treatment used in these applications.

Cysteine Auxotrophic Expression System. The R1 subunit of RDPR has been expressed using the two plasmid T7 RNA promoter/polymerase expression system developed by Tabor and Richardson.[70] The plasmid containing the *nrdA* gene (pMJ1)[4,60] and the plasmid containing the T7 RNA polymerase (pGP1-2) were isolated by standard procedures. They were both transformed into *E. coli* JM15, a strain of *E. coli* auxotrophic for cysteine,[71] and selected on LB plates containing 25 μg/mL ampicillin and 25 μg/mL kanamycin. A single colony was then grown in 5 mL of LB medium[72] or 5 mL of M9 medium[72] supplemented with *L*-amino acids and cofactors.[73] The growth media typically contained in 1 L: 6 g Na_2HPO_4, 3 g KH_2PO_4, 1g NH_4Cl, 1 g NaCl, 5 g glucose, 210 mg $MgCl_2 \cdot 6\ H_2O$, and 14 mg $CaCl_2 \cdot 2\ H_2O$ (pH 7.4 with NaOH), 0.50 g alanine, 0.40 g arginine, 0.40 g aspartic acid, 0.40 g asparagine, 0.4 g glutamine, 0.74 g sodium glutamate, 0.55 g glycine, 0.13 g histidine hydrochloride, 0.24 g isoleucine, 0.23 g leucine, 0.43 g lysine hydrochloride, 0.25 g methionine, 0.15 g phenylalanine, 0.10 g proline, 2.10 g serine, 0.23 g threonine, 0.06 g tryptophan, 0.17 g tyrosine and 0.23 g valine, 0.50 g adenine, 0.65 g guanosine, 0.20 g thymine, 0.50 g uracil, 0.20 g cytosine, 50 mg thiamine, 50 mg nicotinic acid, 100 mg kanamycin and 100 mg ampicillin. Additionally, 120 mg of racemic 3,3,3′,3′-d_4-cystine was added per liter of medium as a suspension in 2 mL of 0.2 M aqueous HCl. A control sample from which the addition of cystine was omitted did not show any bacterial growth, assuring the auxotrophy of our *E. coli* JM15 containing *nrd*A. The 5 mL of culture was grown at 30 °C for 12 h and then used to inoculate 100 mL of the supplemented M9 medium. After another 10 h, this culture was used to inoculate 2 L of the supplemented M9 medium and the cells were grown at 30 °C to an OD_{600} of 1.0 at which point the temperature of the culture was raised rapidly to 42 °C. The temperature was maintained at 42 °C for 1 h followed by an additional 4 h at 37 °C. The cells were then harvested by centrifugation, quick-frozen in liquid N_2 and stored at −80 °C. Protein purification and isolation was carried out as described previously.[4,60] The purified protein had a specific activity of ~1000 nmol min^{-1} mg^{-1}.

9.4 GHz EPR after Incubation of R1 Containing Deuterated Cysteine Residues. A spectrum was recorded of the tyrosyl radical of the R2 subunit before addition of the inhibitor. This sample contained in a final volume of 250 μL: 320 μM R1, 340 μM R2, 0.75 mM TTP, 10 μM TR, 0.5 μM TRR, 0.75 mM NADPH, 15 mM $Mg(OAc)_2$, and 50 mM Tris-HCl (pH 7.6). For instrument settings see the legend with Figure 4. The sample was subsequently thawed and N_3UDP was added in a final concentration of 1.1 mM. The reaction mixture was incubated at 25 °C for 5 min and frozen in liquid nitrogen. A spectrum was recorded using identical instrument settings as used for the sample without N_3UDP.

Interaction of C754/759S R1 with N_3UDP: Analysis by 9.4 GHz EPR Spectroscopy. The inactivation mixture contained in a final volume of 314 μL: 50 mM Tris-HCl (pH 7.6), 15 mM $Mg(OAc)_2$, 100 μM C754/759SR1, 100 μM R2, 20 mM DTT, 1.6 mM ATP and 1.0 mM N_3UDP. The inactivation was started by adding the inhibitor to the protein solution and the mixture was then transferred to an EPR tube and incubated for 8 min at 25 °C. The sample was then frozen and analyzed at 100 K. The EPR settings were identical as described in the legend of Figure 4.

Molecular Modeling. The nonradical structures **C** and **D** depicted below were used as models for the proposed structures **A** and **B** in Scheme 4. Using the QUANTA-CHARMm software package the

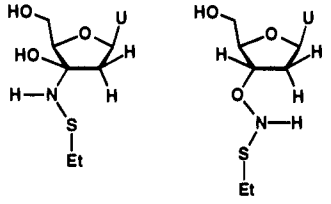

C D

compounds were first energy minimized. The N—S bond was not parameterized in the software, but instead the default parameters for sp^3-hybridized sulfur and nitrogen were used. Then, distance constraints were imposed from the nitrogen atom to the 1′- and 4′-hydrogen atoms based on the ESEEM studies,[16,57] and the structures were again minimized. The distance range from the 2′-hydrogen atom to the nitrogen in the structures obtained was analyzed by rotation along the carbon−nitrogen and nitrogen-sulfur bonds for compound **C** and rotation along the carbon−oxygen, oxygen−nitrogen and nitrogen−sulfur bonds of compound **D**. It should be noted that the distances obtained in the ESEEM studies are experimentally determined and take into account that the unpaired electron is located partly on nitrogen and on sulfur, while the distance constraints used in these molecular modeling studies locate the unpaired electron density completely on nitrogen. Furthermore, these calculations provide minimized structures, while the conformation of the nitrogen based radical inside the active site of RNR will not necessarily correspond to a low energy conformation. We must therefore emphasize that these calculations were carried out for the purpose of providing an estimate of the distance range from the 2′-H to the nitrogen atom in the two model compounds.

Acknowledgment. This research was supported by grants from the National Institutes of Health to J.S. (GM-29595) and to R.G.G. (GM-38352 and RR-00995), by a Jane Coffin Childs postdoctoral fellowship to W.A.v.d.D. (Project 61−960), and an American Cancer Society postdoctoral fellowship to G.J.G. (PF-3668). We thank Dr. J. W. Kozarich (Merck) for a gift of *E. coli* strain JM15 and Prof. J. Peisach (Albert Einstein College of Medicine) for reevaluation of the ESEEM data.

JA9515361

(70) Tabor, S.; Richardson, C. *Proc. Natl. Acad. Sci. U.S.A.* **1985**, *82*, 1074−1078.
(71) Jones-Mortimer, M. C. *Biochem. J.* **1968**, *110*, 589−595.
(72) Sambrook, J.; Fritsch, E. F.; Maniatis, T. *Molecular Cloning A Laboratory manual*; Cold Spring Harbor Laboratory Press: 1989.
(73) Cheng, H.; Westler, W. M.; Xia, B.; Oh, B.-H.; Markley, J. L. *Arch. Biochem. Biophys.* **1995**, *316*, 619−634.